

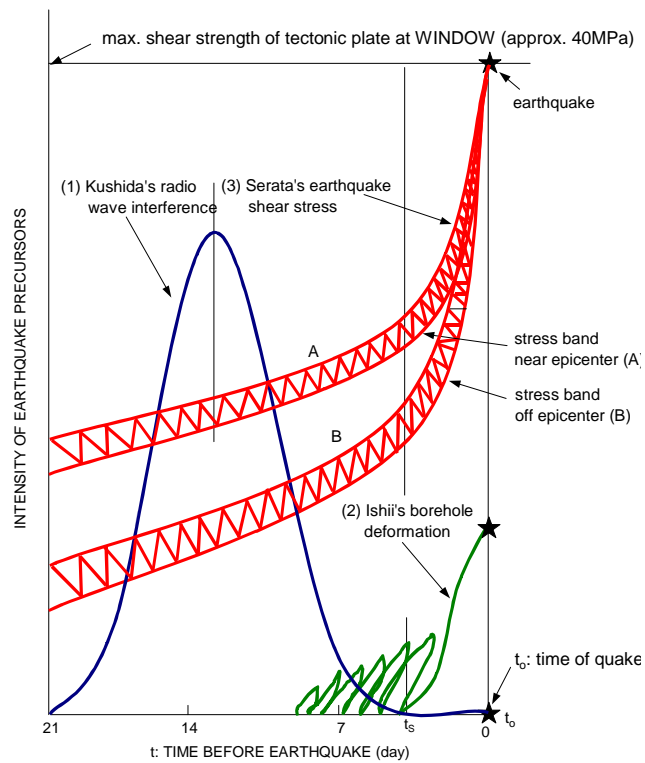


SERATA GEOMECHANICS CORPORATION

Automatic Stress/Property Measurement for Earthwork Optimization

CATEGORY 5 ACCURATE TIME-PREDICTION OF EARTHQUAKES

— Time-Prediction of Forthcoming Major Earthquakes along Shallow Faults —



Serata Geomechanics Corporation

4160 Technology Drive • Fremont • California 94538 USA

Tel: (510) 659-8630 E-mail: serata@serata.com <http://www.serata.com>

Development of Earthquake Time-Prediction Method

Shosei Serata

Serata Geomechanics Corporation

A major advancement in earthquake prediction in California has been made through numerical analysis based on a wide range of geophysical phenomena by the academic and government institutions under NASA's leadership. This development helps us to realize the urgency for time-prediction of forthcoming earthquakes at predicted sites with a sufficient accuracy to save lives.

Completely independent from this development, I, as a geotechnical engineer, accidentally triggered a series of the world's largest man-made earthquakes (magnitude close to 5.0) associated with large-scale underground extraction from the deep potash deposit in Saskatchewan, Canada. From direct measurement of the earthquake stress development in the underground, repeated earthquake occurrences were completely eliminated within 8 months. This elimination was achieved by direct control of the earthquake triggering mechanism and avoided possible abandonment of the extraction operation.

This underground experience was immediately applied to a study of the Hayward fault, which has the highest probability of having a major forthcoming earthquake in the continental U.S. during the next 30 years according to "Probability of Large Earthquakes in the San Francisco Bay Region, California" published by U.S. Geological Survey. While no attention was paid to this study in US, immediately after the Kobe earthquake of 1995, an urgent request was received from the Japanese government to introduce Serata Stress Technology (SST) with its Stress Probe to Japan.

To support this development in Japan, extensive studies were carried out in US and Canada that successfully formulated a practical method for accurate time-prediction of forthcoming major earthquakes at predicted sites with engineering certainty. This development is an outgrowth of the following four evolving processes.

- Discovery of Intrinsic Gradient of Lateral Tectonic Stresses, σ_H and σ_h
- Discovery of Constant Tectonic Shear Stress, τ_o^E
- Hypothesizing of Earthquake Stress Cycle
- Field Verification of the Hypothesis to Achieve Time-Prediction

1. Introduction of SST to Japanese Government Program

Accidental triggering of the Saskatchewan earthquakes led us to the understanding that maximum shear stress that exceeded the maximum shear strength of a critical stratum, is the direct cause of forthcoming earthquakes. When excavation of the deep potash deposit was started during the 1960's and 1970's at eight different locations in Saskatchewan, all of the mining operations suffered major ground failure due to high stress concentration, relative to the strength of ground, around their working openings. Because the failures were intense and rapid, some of the operations were about to be abandoned completely during initial development stages before the start of full production. Possible losses were on the order of one billion dollars for each operation. Accurate stress measurement of the failing ground enabled us to overcome the failures by invention of the "Stress Control Method" by S. Serata. Details of this development are described in Category 4 "Earthwork Application Examples" in this website.

It became apparent that the Saskatchewan earthquakes were caused by an engineering mistake in the application of "Stress Control Method" to the mining ground, which is illustrated in Fig. 5-1. The engineering method to stop the earthquakes was very simple. It was to reduce the maximum shear stress along the failing shear plan, which was accomplished by reducing the critical stress by widening the spacing between "Panel Stress Envelopes" from 100m to 130m. This reduced the maximum earthquake triggering stress by 23%, which was sufficient to stop the repeating earthquakes.

The initial triggering of the earthquakes attracted a great interest from the Geophysics Department of University of Saskatchewan, located within ten miles from the earthquake site, in Saskatoon, Saskatchewan. A major research program was planned by the Department, but there was no need to execute it because the earthquake triggering mechanism was totally eliminated before the program went into effect. Documentation of this event is still kept in the Department Library.

Success of the Saskatchewan earthquake prevention project inspired our interest to study possible time-prediction of forthcoming major earthquakes along the Hayward fault, which is runs through heavily populated parts of the San Francisco Bay Area, as illustrated in Fig. 5-2. The probability of occurrence of forthcoming earthquakes along the fault has been considered the highest in the continental US, according to U.S. Geological Survey. Even though we did not conducted stress measurements along the fault, the currently existing earthquake shear stress τ_o^E on top of the tectonic plate is estimated by utilizing existing creep and seismic data available from U.S.G.S. as shown in the figure. This engineering

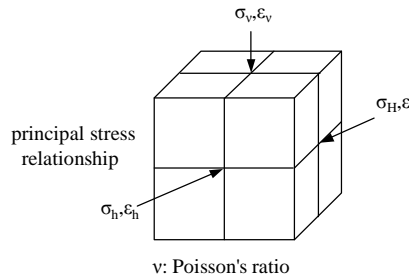
approach by Serata Stress Technology (SST) was invited to participate in a Japanese government earthquake study program immediately following the Kobe Earthquake of 1995.

2. Intrinsic Gradient of Lateral Tectonic Stresses ($\Delta\sigma_H/\Delta\sigma_v$ & $\Delta\sigma_h/\Delta\sigma_v$)

The Japanese government program provided a springboard for SST to get involved in earthquake stress measurement in Japan. Principles and field verifications of Serata Probe are explained in detail in Categories 1, 2 and 3 in this website. The most important application of the Probe was participation in a national competition on stress measurement organized by Ministry of Economics & Industry of the Japanese government. The competition was held under the supervision of Officer Koide at the National Testing Ground in the foothills of Mt. Fuji, about 100 km west of Tokyo. Four stress-measurement methods, (1) overcoring, (2) hydrofracturing, (3) deformation and (4) Serata were carried out by four different geotechnical companies participating in the competition. Their overall measurement results, achieved within a strict time limit of one day, are compared in Fig. 5-3.

Similar test results were expected from the four different methods because of uniform stress condition of the test ground. Actual results differed significantly disclosing a serious unreliability of the stress-measurement methods as a whole. A careful study of the confusing results led to the clear conclusion that the Serata method is the only competing method that reliably shows the actual stress condition of the ground. This conclusion is based on the following observations:

- 1) Measurement Efficiency: Serata method is efficient enough to complete six measurements at six different depths in the allotted time (one day) while the other methods were barely able to complete one measurement at their respective starting depths.
- 2) Maximum Lateral Stress (σ_H): The six σ_H -values obtained at the six elevations by Serata method fall upon a straight gradient line of $\tan \theta = 0.25$.
- 3) Minimum Lateral Stress (σ_h): The σ_h -value obtained at the six elevations also fall upon a straight line parallel to the σ_H line of $\tan \theta = 0.25$.
- 4) Depth Gradient Value ($\tan \theta$): These parallel depth gradient lines are in excellent agreement with the theoretical value of the lateral tectonic stress gradient of $\tan \theta = 0.25$, which S. Serata derives as follows.



Generalized underground stress-stain relationship is given by the elasticity relation:

$$\left. \begin{aligned} E \cdot \epsilon_v &= \sigma_v - \nu (\sigma_H + \sigma_h) \\ E \cdot \epsilon_H &= \sigma_H - \nu (\sigma_h + \sigma_v) \\ E \cdot \epsilon_h &= \sigma_h - \nu (\sigma_v + \sigma_H) \end{aligned} \right\} \dots\dots\dots (1)$$

By increase of depth, we get $\epsilon_H = \sigma_h = 0$, then:

$$\left. \begin{aligned} \Delta \sigma_H &= \nu (\Delta \sigma_h + \Delta \sigma_v) \\ \Delta \sigma_h &= \nu (\Delta \sigma_v + \Delta \sigma_H) \end{aligned} \right\} \dots\dots\dots (2)$$

Eq. 2 leads to the depth gradient as:

$$\tan \theta = \Delta \sigma_H / \Delta \sigma_v = \Delta \sigma_h / \Delta \sigma_v = (\nu + \nu^2) / (1 - \nu^2) = 0.24 / 0.96 = 0.25 \dots\dots\dots (3)$$

here, $\nu = \text{Poisson's ratio} = 0.2$

The nearly perfect agreement of the Serata measurements with the theoretical value is a positive proof that Serata method is effective and accurate. Unexpectedly, this led to opening up a new possibility of "Engineering Approach" toward direct and automatic measurement of lateral tectonic shear stresses at a rather shallow depth on top of the tectonic plate as explained next.

3. Discovery of Constant Tectonic Shear Stress

The previous observation led to an important discovery related to lateral tectonic shear stress in any ground, i.e. in an undisturbed stratum, the intrinsic lateral tectonic shear stress remains constant and is unaffected by depth change. Consequently, the following mathematical relationship to exists in the underground even near the surface.

$$\Delta \tau_o / \Delta \sigma_v = (\Delta \sigma_H - \Delta \sigma_h) / 2 \Delta \sigma_v = 0 \dots\dots\dots (4)$$

This means that lateral tectonic shear stress is unaffected by depth. Because of the great importance of this finding to our earthquake triggering study, validity of the finding at the Mr. Fuji site was re-examined by repeating similar measurements at various locations in Japan. It was a quite surprise to obtain exactly the same results everywhere in Japan that validated the reality of the intrinsic lateral stress gradient as mathematically derived in Eq. 3. At the same time, it was discovered that the constant gradient line shifts laterally at certain strata boundaries frequently, resulting in much greater apparent gradients as shown in Fig. 5-4. A most dramatic shift is found in the data obtained from a hydrofracturing test, conducted by the late Y. Tanaka of Kyoto University at Mannari, Okayama, Japan, that demonstrates a large shift in a major soft disturbed stratum at a depth of 200m (see Fig. 5-5). This type of sudden large shift is found to be the rule rather than an exception because it is observed everywhere that we have studied in the world as discussed below.

Based on analysis of the data from Japan to a depth of 300m, a similar analysis, of tectonic stress state was extended to greater depths (to 4,000m). This study utilized data obtained from various major international programs. Fig. 5-6 illustrates stress data obtained by an English Dry Hot Rock Program, using the hydrofracturing method, to a depth of 2,000m in the Carmenellis granite at Cornwell, England. These data support the findings of the Japanese work very well. Similar relationships are found in the Canadian granite shield at Timmons, Ontario (Herget, et al) to the depth of 2,000m as illustrated in Fig. 5-7.

At a depth of about 2,000m, the overburden weight starts increasing the lateral stress gradient value toward $\tan \theta = 1.0$ as demonstrated by the Hot Dry Rock Program in Fenton Hill, New Mexico and by a KTB project in Germany as shown in Figs. 5-8 and 5-9, respectively. Even though lateral stresses σ_H and σ_h vary widely in relation to depth, location and geology, the fundamental characteristics of stress state are found to be consistent enough to arrive at the following significant characterization of the global tectonic stress state.

- 1) Depth Gradient: Depth gradients of σ_H and σ_h to depths of about 2000m are always constant at values near the intrinsic value of $\tan \theta = 0.25$ indicating that the ground is not readily yielding until this depth is reached.
- 2) Shifting Gradient: Even though the lateral stress gradient remains at the small intrinsic value to 2,000m, the gradient line to depths of 500m to 600m makes frequent parallel shifts resulting in a large apparent gradient value as shown by "Surface Effect" in Fig. 5-10. The gradient shifting usually ends at these shallow depths, resulting in a set of well-defined parallel intrinsic gradient lines of $\tan \theta = 0.25$.

- 3) Region of Earthquake Shear Stress τ_o^E : After ending the frequent shifting around the depth of 500m, both gradients of σ_H and σ_h usually settle at the intrinsic value, resulting in a pair of straight parallel gradient lines of σ_H and σ_h , showing a constant lateral shear stress value, from which the truly acting (real) earthquake shear stress $\tau_o^E = (\sigma_H - \sigma_h)/2$ is derived as shown in Fig. 5-10.
- 4) Window for τ_o^E Measurement: The above condition usually continues to a depth of about 2,000m, beyond which the gradient starts shifting toward the geostatic value of $\tan \theta = 1.0$ due to gravity overwhelming the strength of the rock media slowly but definitely. The top of this constant τ_o^E region (500 ~ 2,000m) is defined here as "Window" where earthquake stress ($\tau_o = \tau_o^E$) can be measured and monitored most accurately and economically.

4. Hypothesis of Earthquake Stress Cycle

From the above observations on lateral tectonic stress in general, the following mechanism of earthquake stress cycle is proposed. This is a hypothesis, to be examined, tested and improved, developed to achieve time-prediction of forthcoming major earthquakes. This hypothesis is based on the two major precursors, which were established in Japan following the Kobe earthquake of 1995. One is electromagnetic interference on FM radio wave usually observed a few weeks prior to a major (shallow) earthquake and the other is micro-strain in shallow wells observed one week prior to the major earthquakes. Both precursors must reflect yielding of the ultimate stress nucleus where the final rupturing process begins a few weeks prior to occurrence of the earthquake. This hypothesized process is based on the following six basic geomechanical interpretations of stress nucleus yielding.

- 1) Stress State at Greater Depth: Stress state at greater depth (to 14,000m) is estimated in Fig. 5-11, which illustrates a five-stage earthquake stress cycle expected to take place in the ultimate stress nucleus at the epicenter. This illustrates the principal stress distribution across the entire depth with five stages of development to final rupture.
- 2) Earthquake Shear Stress Cycle: The principal stress cycle is converted to a tectonic shear stress (τ_o) cycle at the ultimate stress nucleus as shown in Fig. 5-12.
- 3) Ultimate Shear Yielding: Finally, yielding of the matured nucleus brings the earthquake shear stress τ_o^E -value across the entire thickness of the plate in order to trigger the major earthquake. This final process of the shear failure is indicated by the

step from (4) to (5) as shown in Fig. 5-12.

- 4) Two Major Precursors: In this final yielding process, through the entire earthquake shear plane, two major earthquake precursors are released as shown in Fig. 5-13. One is the electromagnetic interference in the ionization zone in the sky as established by Y. Kushida and the other is borehole micro-strain established by H. Ishii. They are entirely different phenomena originating from the same ultimate yielding of the stress nucleus.
- 5) τ_o^E and Two Precursors: The earthquake stress τ_o^E build-up at Window is another phenomenon caused by shear yielding of the nucleus, which is superimposed on the previously discussed precursors in the figure (Fig. 5-13). A set of two simultaneous stress measurements (A & B) is presented by two bands (A & B), which are τ_o^E readings that would be obtained from two Stress Probes. The Probes are located in the nucleus along the prospective fracture plane of the fault as illustrated by the FEM model of stress nucleus given in Fig. 5-14. Probe A is located closer to the epicenter than Probe B, therefore, A-band increases sooner than B-band, even though both bands eventually show failure at the time of the rupture. This is the final part of the earthquake cycle, which needs to be field validated.
- 6) Accuracy of Time-Prediction: The τ_o^E observation is represented by the two different stress belts with daily cycles characteristic of earth tide effects. Because, each stress probe measurement can be repeated more than 50 times daily, a high accuracy of time-prediction in terms of hours and minutes is considered possible with engineering certainty.
- 7) Field Verification of Hypothesis: The above hypothesis of earthquake prediction by τ_o^E monitoring can be directly examined by measuring the earthquake stress τ_o^E at Window. The present earthquake stress τ_o^E at the epicenter of the 1995 Kobe quake (Nojima) must be very small (less than 10 MPa) while the stress at Ashio earthquake district, where repeated quakes are now occurring, must be close to the upper limit (40 MPa). The Japanese government study program by Environmental Protection Science and Technology Institute headed by R. Ikeda examined these contrasting conditions by measuring the earthquake stresses at Window at the two sites, respectively. Results of their measurements demonstrate validity of Serata's hypothesis on earthquake stress τ_o^E rather accurately as shown in Fig. 5-15. In the same figure, these Japanese measurement results are compared with data from Cajon Pass, California (by Mark Zoback et al), which is an interesting case where there are large lateral stresses (σ_H and σ_h) and a small possibility of horizontal shear failure. Field operation is illustrated

by the schematic diagram and photograph given in Figs. 16 and 17.

5. Discussion

The geomechanical method for time-prediction of forthcoming major earthquakes is formulated as an outcome of a long series of R&D efforts over the past 35 years. The following four consecutive stages of developments are discussed for the purpose of initiating a dialog on this new stress technique and how it can be incorporated into the main stream of earthquake studies.

- 1) Innovation of Automatic Stress Probe: The innovation of Stress Probe was originally made to develop a safe method for ultimate disposal of the nation's high-level nuclear waste in the underground (see Category 3). The forerunner to the studies was a series of large man-made earthquakes (magnitude 5.0) triggered by a geomechanical error in "Stress Control" of excavation in a deep underground potash mine in Saskatchewan, Canada. The recurring earthquakes were totally stopped by reducing the critical shear stress of the underground by 23%. These geomechanical events disclosed that the direct cause of the shallow earthquakes was an increase of shear stress beyond the minimum strength of the critical shear plane. Serata Stress Probe, invented for the mine study, can be useful for earthquake stress monitoring in general and for earthquake time-prediction in particular. Specifically, the Probe, based on the force-balance principle of single-fracture method, has successfully overcome the accuracy and operational constraints of conventional stress-measurement methods as summarized in Table 5-1. The details of the Probe are given in Categories 1, 2 and 3 of this website.
- 2) Discovery of Earthquake Stresses, τ_o^E : As soon as Stress Probe was introduced to Japan, it discovered that intrinsic lateral tectonic stress gradient near the surface is constant at the value of $\tan \theta = \Delta\sigma_L/\Delta\sigma_v = \Delta\sigma_H/\Delta\sigma_v = \Delta\sigma_r/\Delta\sigma_v = 0.25$. This finding was verified to be true globally to depths greater than 2,000m by evaluation of stress data obtained from international deepwell stress-measurement programs. A consistency of all these findings led to the geomechanical definition of earthquake stress τ_o^E .
- 3) Hypothesis of Earthquake Cycle with Window: In order to relate τ_o^E -value to the triggering moment of forthcoming earthquake, a hypothesis on earthquake stress cycle, based on geomechanics principles, is proposed to enable time-prediction.
- 4) Verification of Hypothesis: The above hypothesis was tested and proven to be accurate

enough for practice of time-prediction by Japanese government programs. Even though, this is the first and only validation of the hypothesis, the agreement between the hypothesis and the measurements made in the two different Japanese earthquake sites is excellent.

5) Best Conceivable Approach

The preceding findings and developments are not sufficient to prove the hypothesis but they do indicate that it may have validity. Because this is the only known hypothesis with a possibility to realize time-prediction of forthcoming earthquakes, it deserves further study.

6) Acceptance in Japan

Usefulness of the Technology is verified by the official adoption of the Technology to the latest research programs of both the Earthquake Research Institute of Tokyo University and the Earthquake Prediction Program of National Research Center of the Japanese government.

6. Conclusion

This study shows that Serata Stress Technology with the Probe has the potential to achieve time-prediction of forthcoming major earthquakes at predicted sites with engineering certainty. This conclusion is based on a unification of the following four innovations.

- 1) Stress Probe made to measure earthquake shear stress automatically as a function of time with repeatability of more than 50 measurements per day.
- 2) Engineering methodology of earthquake stress monitoring with the Probe at Window on the top of tectonic plate at shallow depth range of 500m to 1,000m.
- 3) Geomechanical model of the major earthquake stress cycle enabling high accuracy time-prediction.
- 4) Proprietary “stress transparent” borehole boundary permanently protected for long-term repeated stress measurements in deteriorating ground.

7. Acknowledgements

Dr. John Labrecque of NASA provided me guidance and encouragement to continue this effort. Extensive fieldwork with the Stress Probe in Japan was carried out over 15 years by S. Sakuma, former Technical Director of JDC Corp. Results of recent stress-measurement work at Nojima and Ashio were provided by R. Ikeda and A. Cho of

the Japanese government research institutes. Preparation of this paper is made possible by the dedicated contributions in evaluation and editing of the draft by W. Haenggi, former Chief Geologist of The Dow Chemical Company.

8. References

References are given in Category 6 “Global Project Records and References” in this site.

For further information contact Shosei Serata at serata@serata.com or (510) 659-8630 / (510) 797-4228.

Table 5-1

Serata Stress Method Compared with Conventional Methods

Category \ Method	Hydrofracturing Method	Overcoring Method	Serata's Single-Fracture Method
Simultaneous Measurement of In-situ Material Properties with Stress Measurement	not possible	not possible	yes, automatically done
Repeating Stress Measurement in Relation to Time at Same Position	not possible	not possible	Yes automatically done
Speed of Measurements (measurement/day)	usually one measurement/day in shallow depth	taking days and week for greater depth	10 ~ 50 measurements/day
Automation of Measurement, Analysis & Graphic Display on Site	not possible	not possible	yes. all done on-site in real-time
Requirement of Separate Supporting Tasks	high-pressure packing, water injection & fracture indentation	probe cementation, overcoring & specimen recovery	none at all
Requirement of Core Specimen Recovery and Laboratory Testing	yes	yes	no
Dependence upon Hypothesis of Elasticity of Ground	yes	yes	not at all
Applicability to Complex Ground	not possible	not possible	applicable
Accuracy in Stress Measurement	± 10 ~ 20% often not possible	± 10 ~ 20% often not possible	± 2% or better as needed
Price/Measurement Including Property Testing	\$2,000 ~ \$6,000 dependent upon depth	\$1,000 ~ \$4,000 depend upon depth	\$200 ~ \$800 unaffected by depth
Overall Efficiency (Accuracy)x(Speed) x (Repeat) & Future Potential	1 very little	1 very little	a few order of magnitude greater sole domination globally

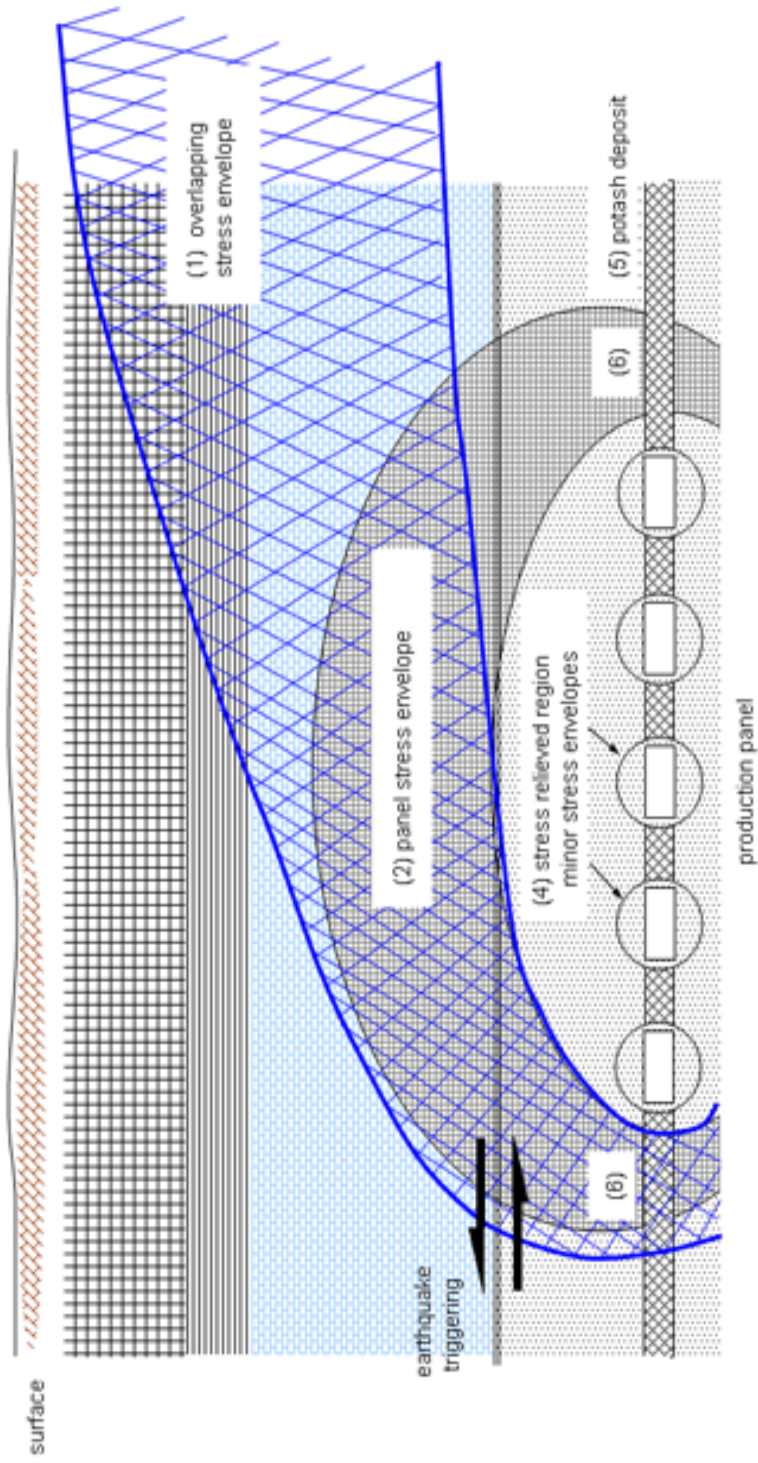


Fig. 5-1 Stress Control Method applied to stabilize deep underground openings that went out of control and caused series of major earthquakes (magnitude 5.0) by rupturing in major weakness stratum overlying potash deposit in Saskatchewan, Canada

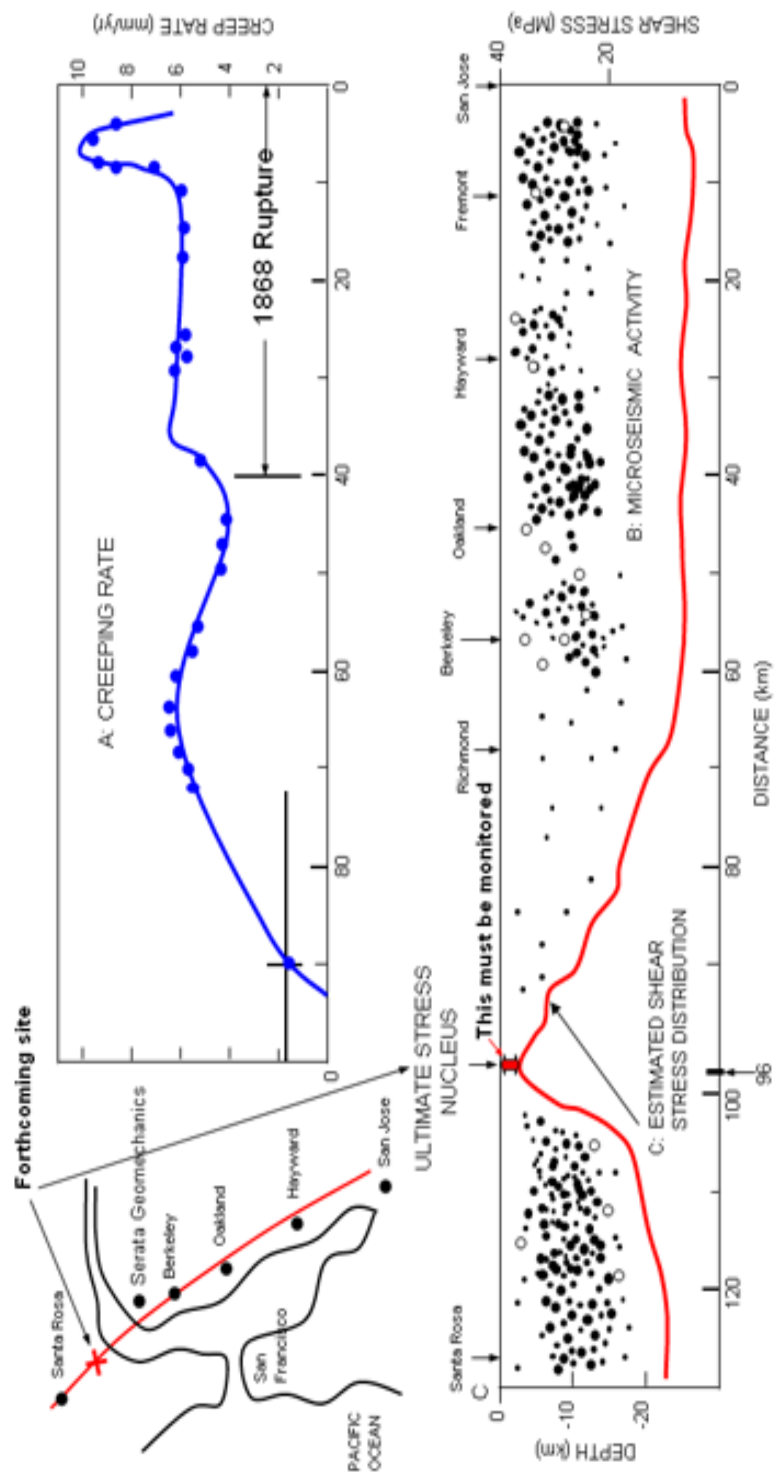


Fig. 5-2 Distribution of (C) earthquake (shear) stress, estimated from (A) distribution of creep rate and (B) microseismic activities found along Hayward fault in San Francisco Bay Area indicating site of the forthcoming major earthquake where tectonic stress build-up should be monitored continuously.

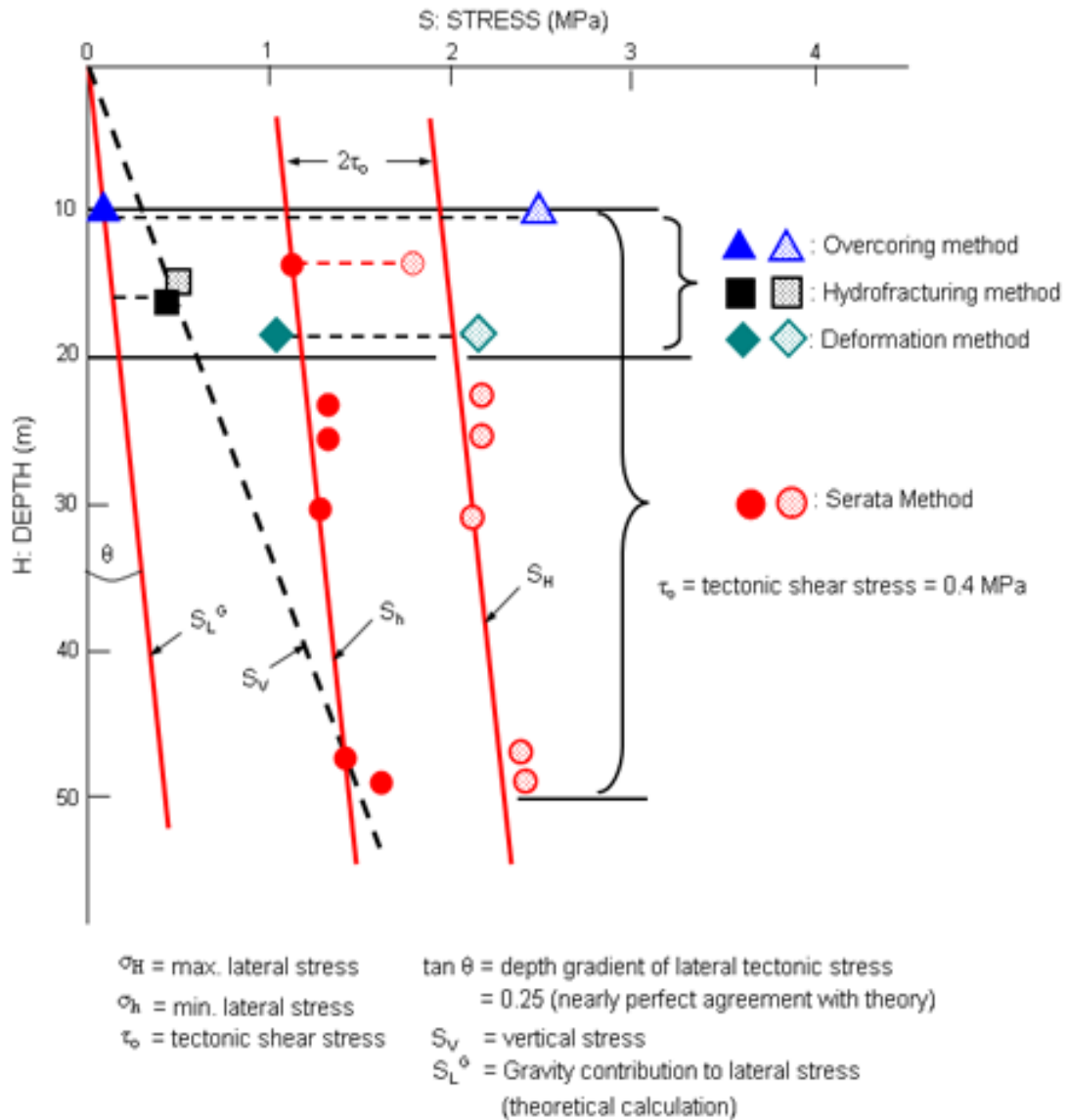


Fig. 5-3 Results of the national competition on tectonic stress measurements conducted at Mt. Fuji Test Site by Ministry of Economics and Industry of Japanese government, demonstrating distinction of Serata Method, capable of completing multiple measurement to 50m in the day allocate for testing

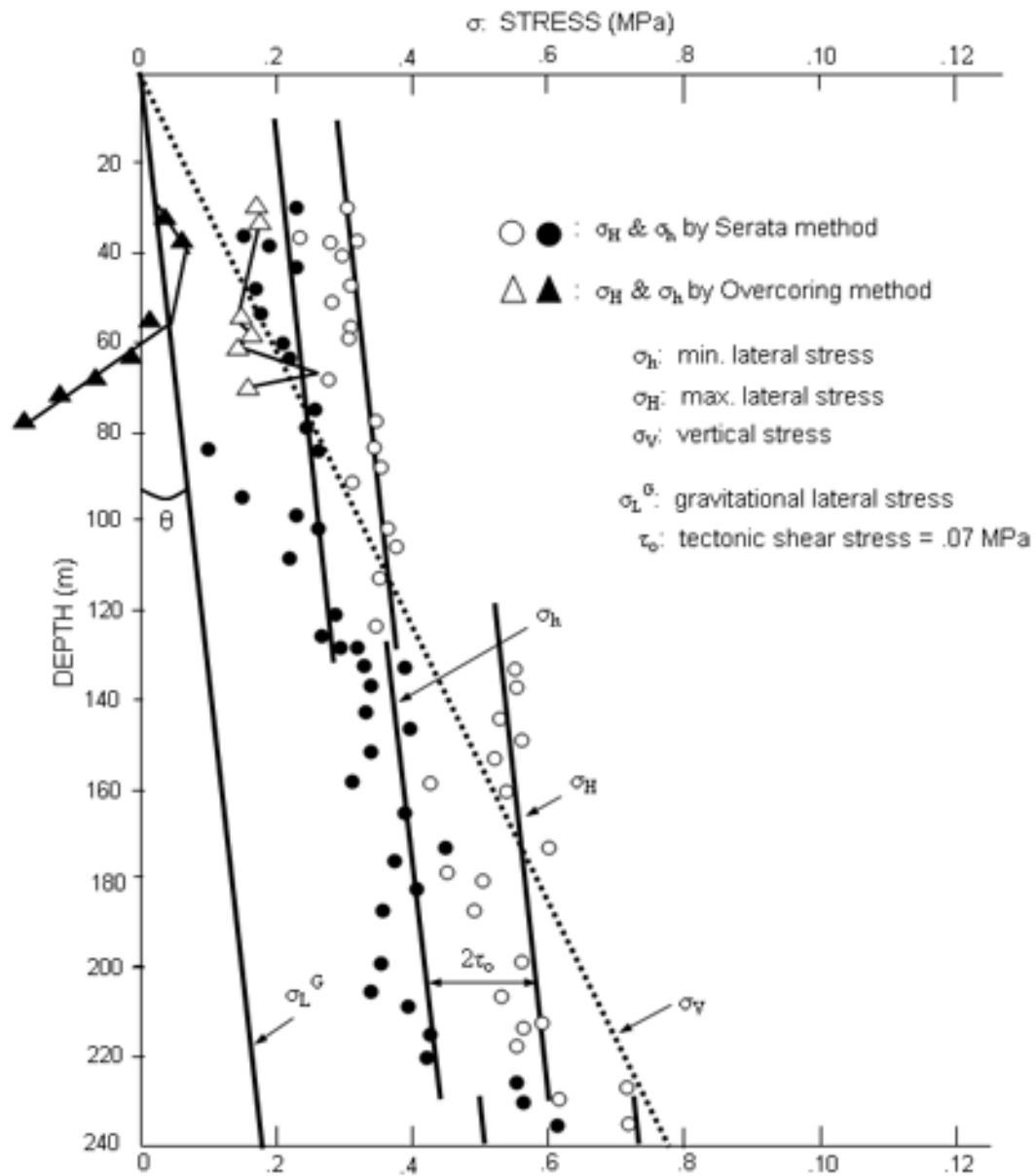


Fig. 5-4 Lateral stresses measured by Serata method and overcoring method in fractured green schist formation in nuclear power plant foundation in Shikoku, Japan, showing constant depth gradient of $\tan \theta = 0.25$. Note the difference between two methods applied to the same ground, which is commonly observed

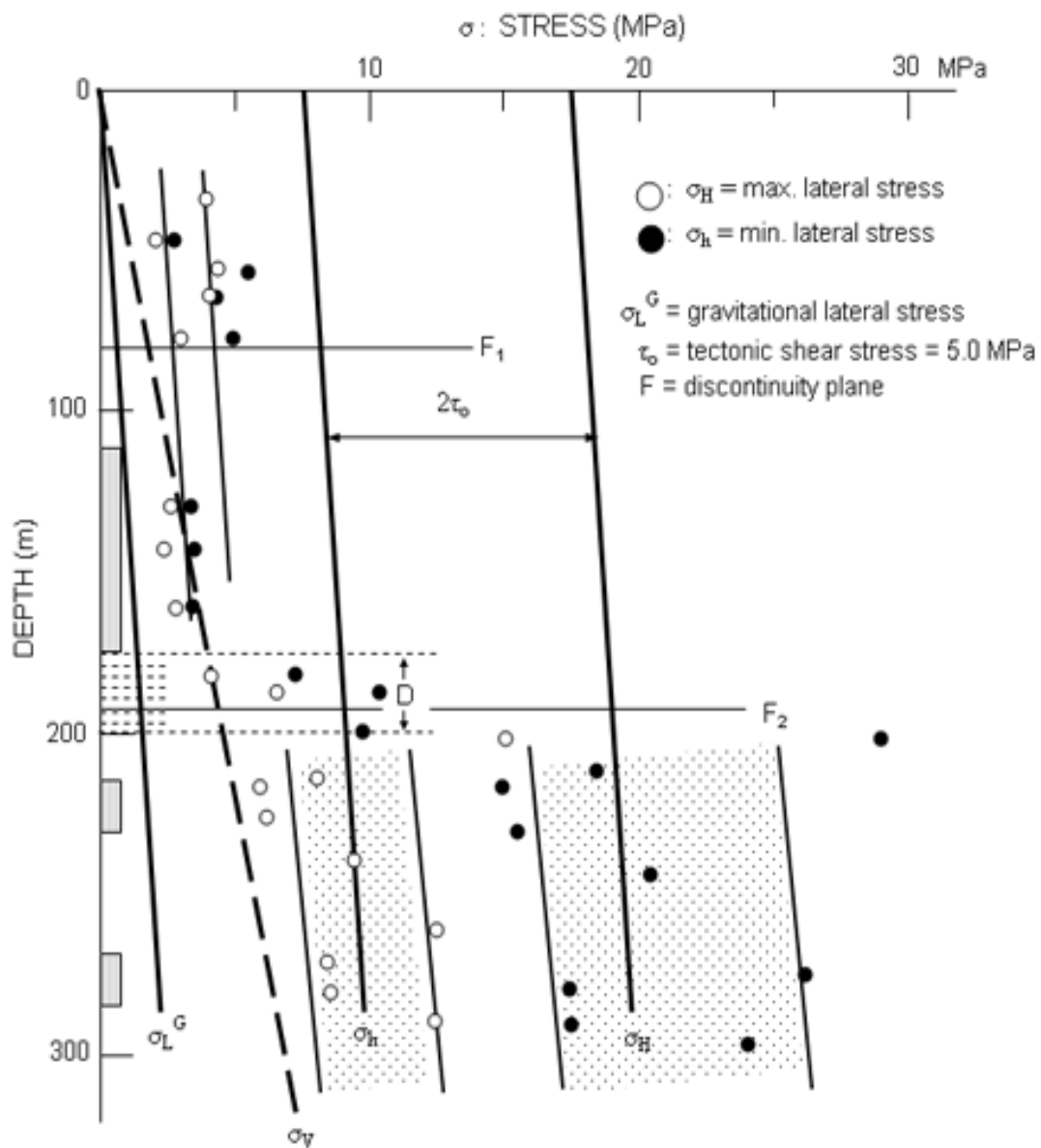


Fig. 5-5 Depth distribution of lateral stresses at Mannari, Okayama, Japan obtained with hydrofracturing method by Y. Tanaka, σ_L^G , and τ_0 are added by Serata showing the same stress gradients of σ_L^G for σ_H and σ_h even across major discontinuity planes

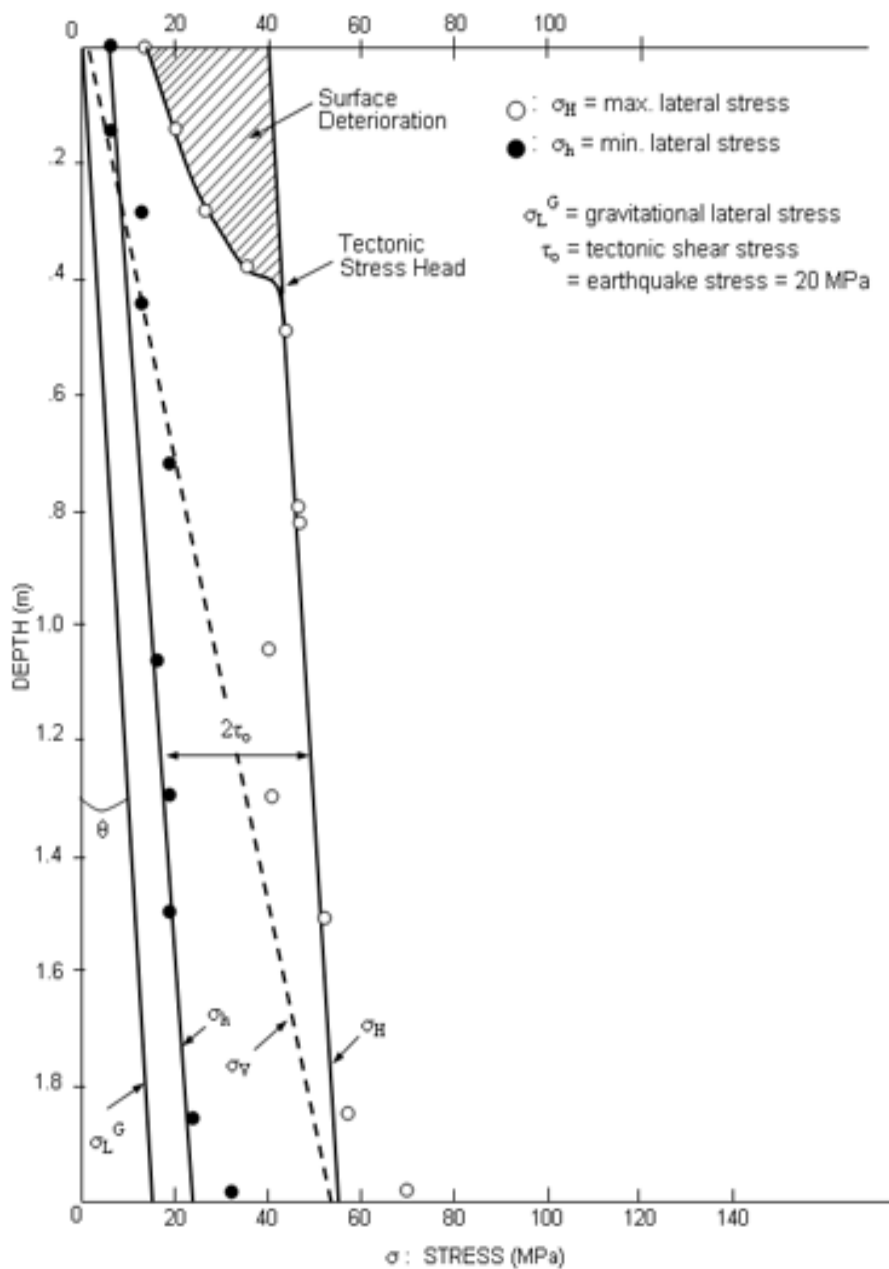


Fig. 5-6 Interpretation of stress data obtained from English Hot Dry Rock Project in Carmenellis granite, Cornwall, England by Pine and Batchelor (1982). τ_0 , σ_V , σ_L^G , $\tan \theta$ and shaded area are added by Serata.

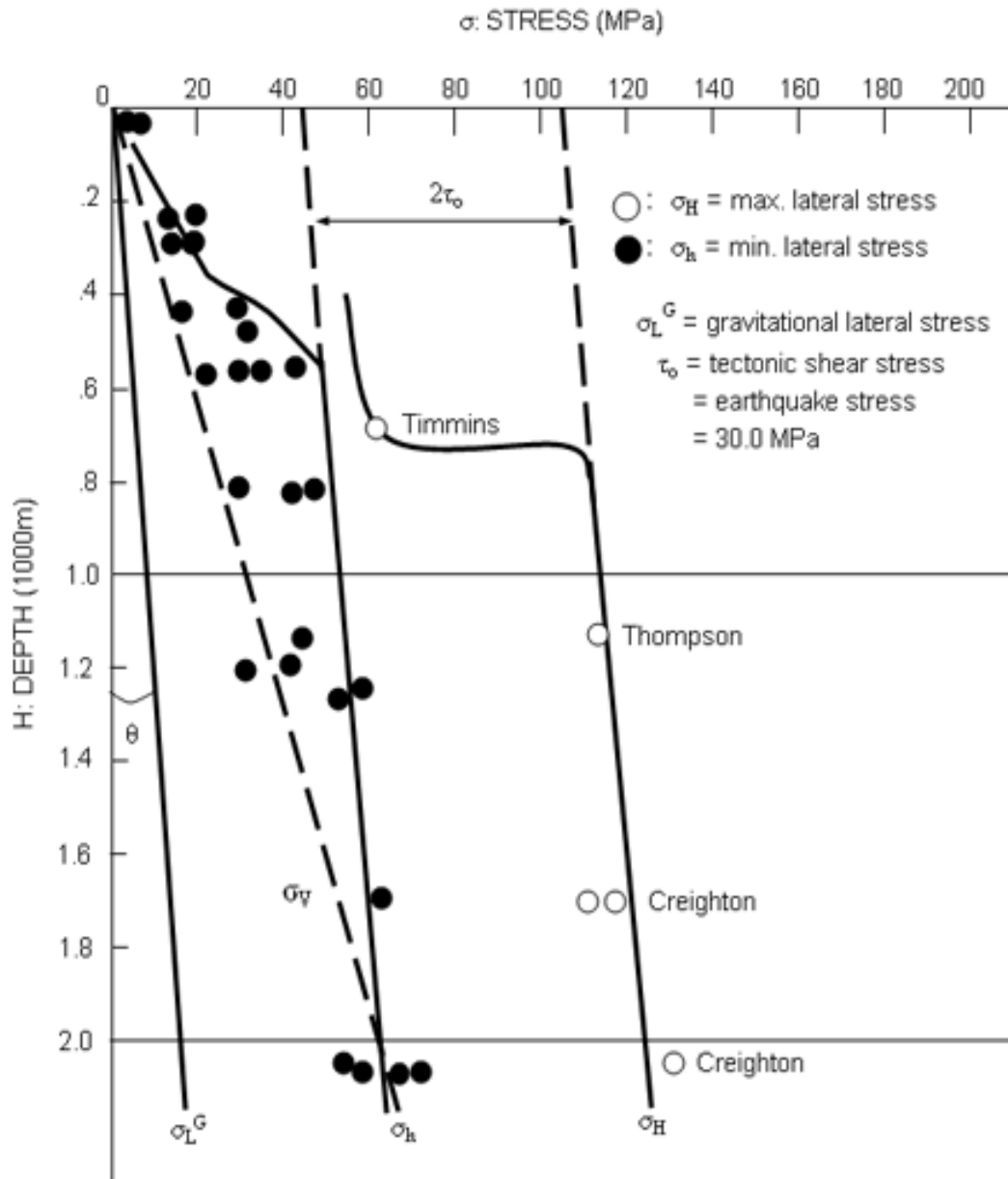


Fig. 5-7 Depth distribution of lateral stresses obtained from three deep mines of the Timmins Mining District in Canadian Shield, Contribution from Herget (1982). σ_L^G and τ_0 are introduced by Serata.

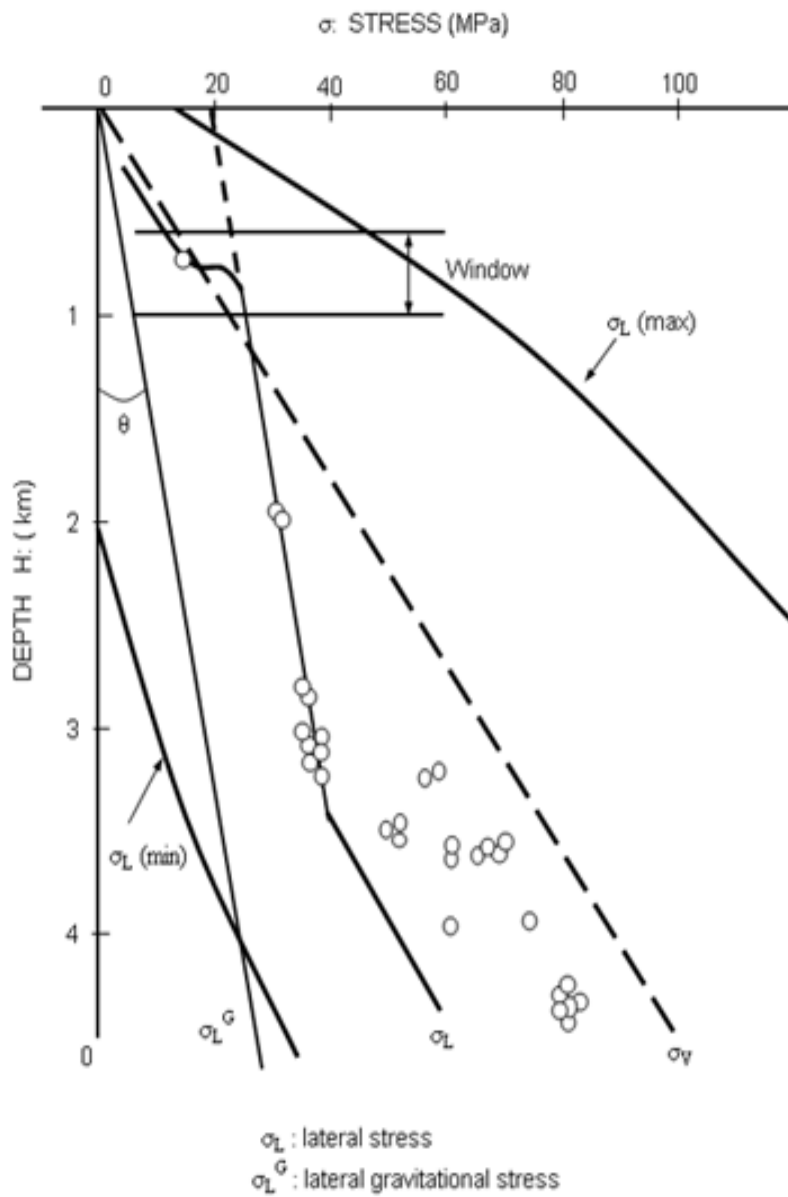


Fig. 5-8 Interpretation of deep stress data by hydrofracturing method obtained at Fenton Hill, New Mexico by Hot Rock Program of Los Alamos National Laboratory (1987). σ_L (min), σ_L (max) and σ_L^G are added by Serata.

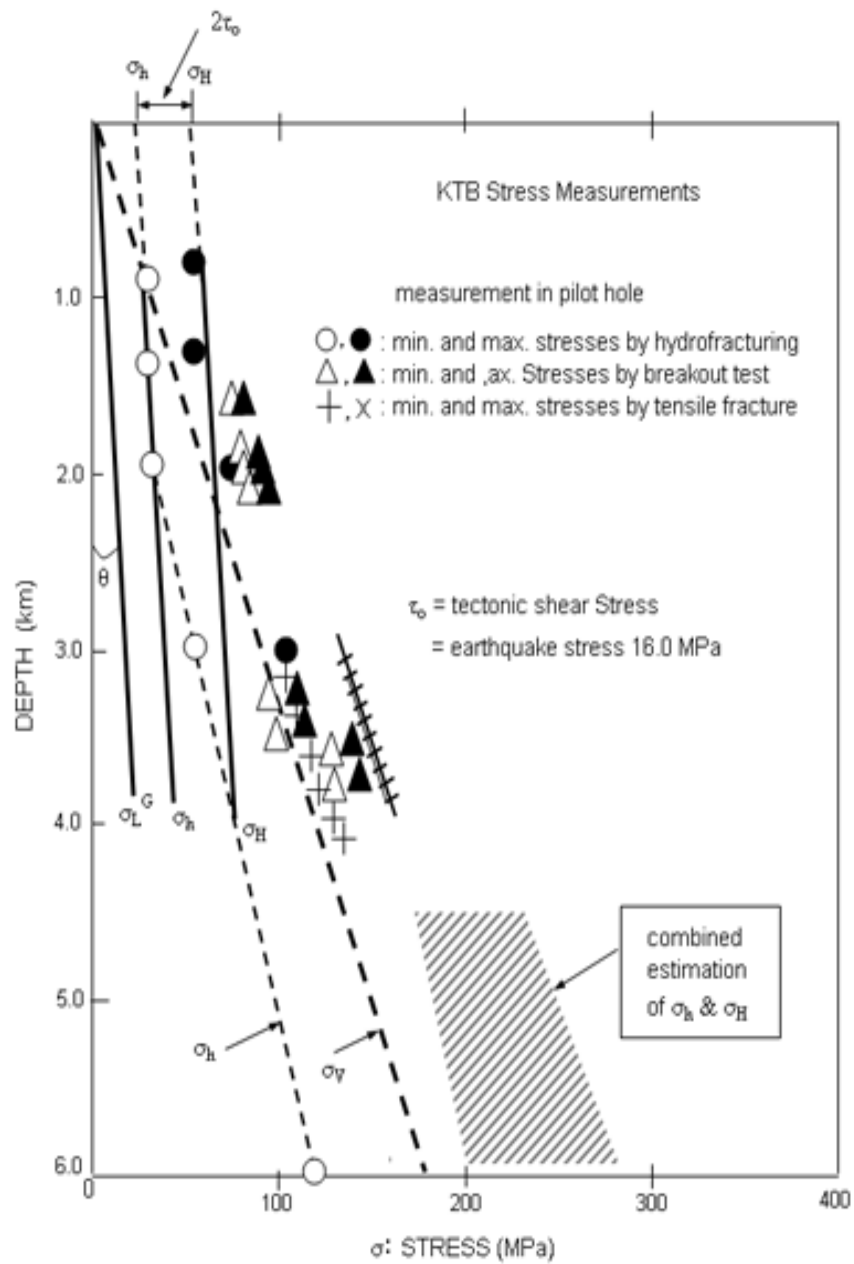


Fig. 5-9 Distribution of lateral stresses obtained from hydrofracturing and borehole breakout methods in the KTB tests by Vermeik et al (1982). The gravitational lateral stress σ_L^G and τ_0 are added by Serata.

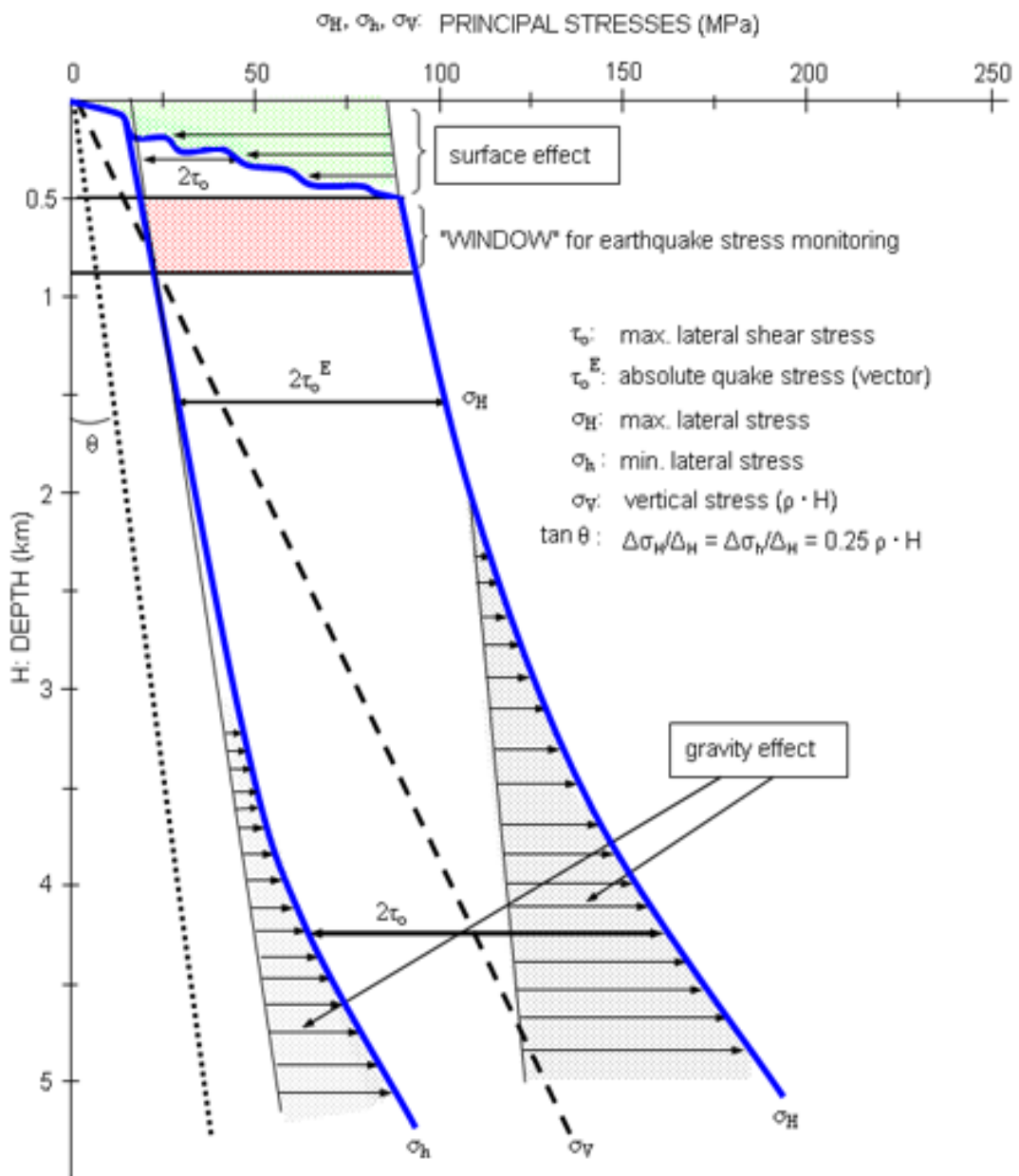


Fig. 5-10 Depth distribution of principal stresses, illustrating relations among tectonic stress tensor (σ), earthquake stress vector (τ_o^E) and window for τ_o^E measurement.

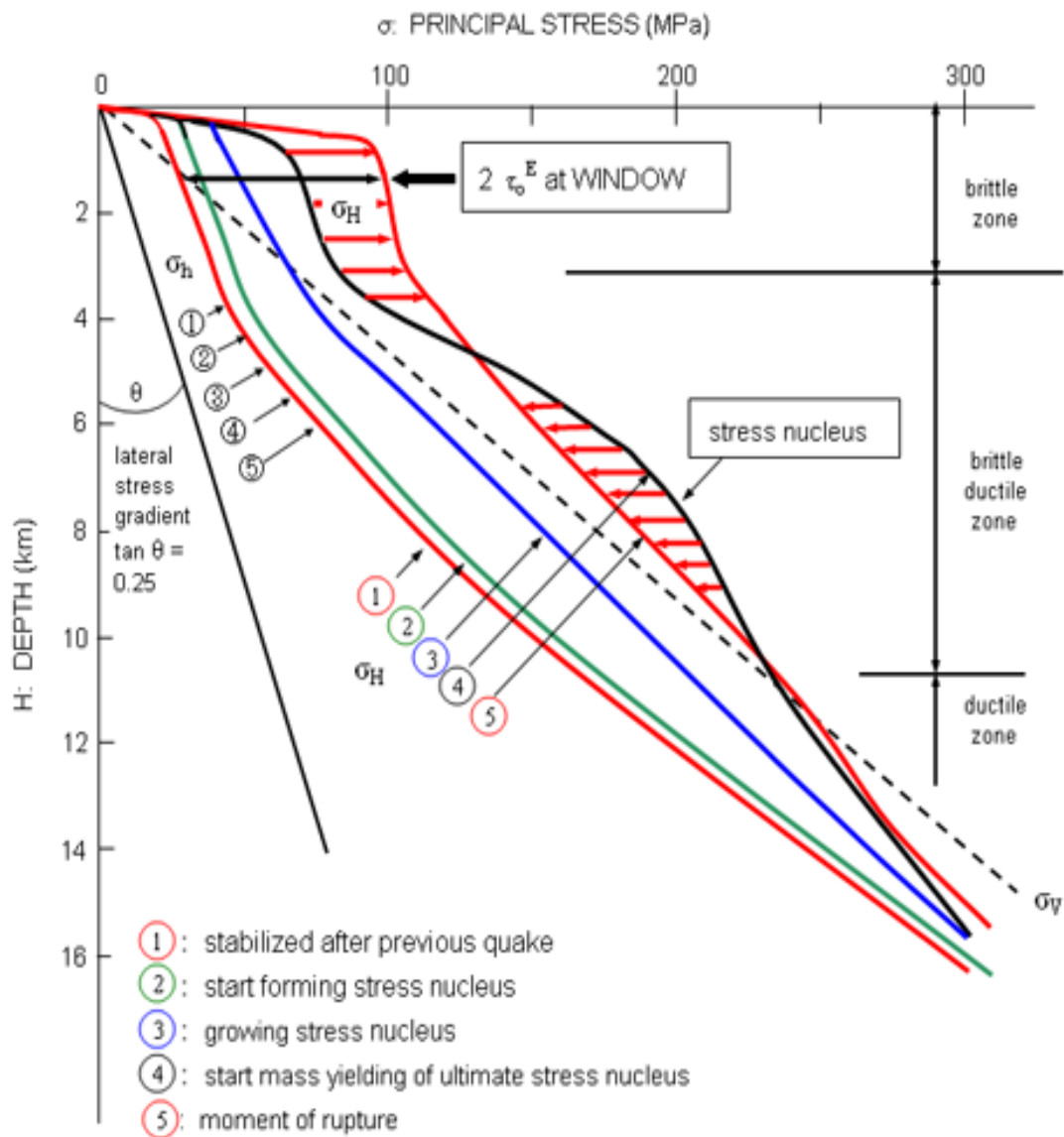


Fig. 5-11 Depth distribution of σ_H & σ_h in relation to 5 stages of earthquake stress cycle through stress nucleation illustrating massive yielding and rise of earthquake shear stress τ_o^E at Window. Window is defined as top of tectonic plate where τ_o^E -value is measured at minimum required depth as indicated here

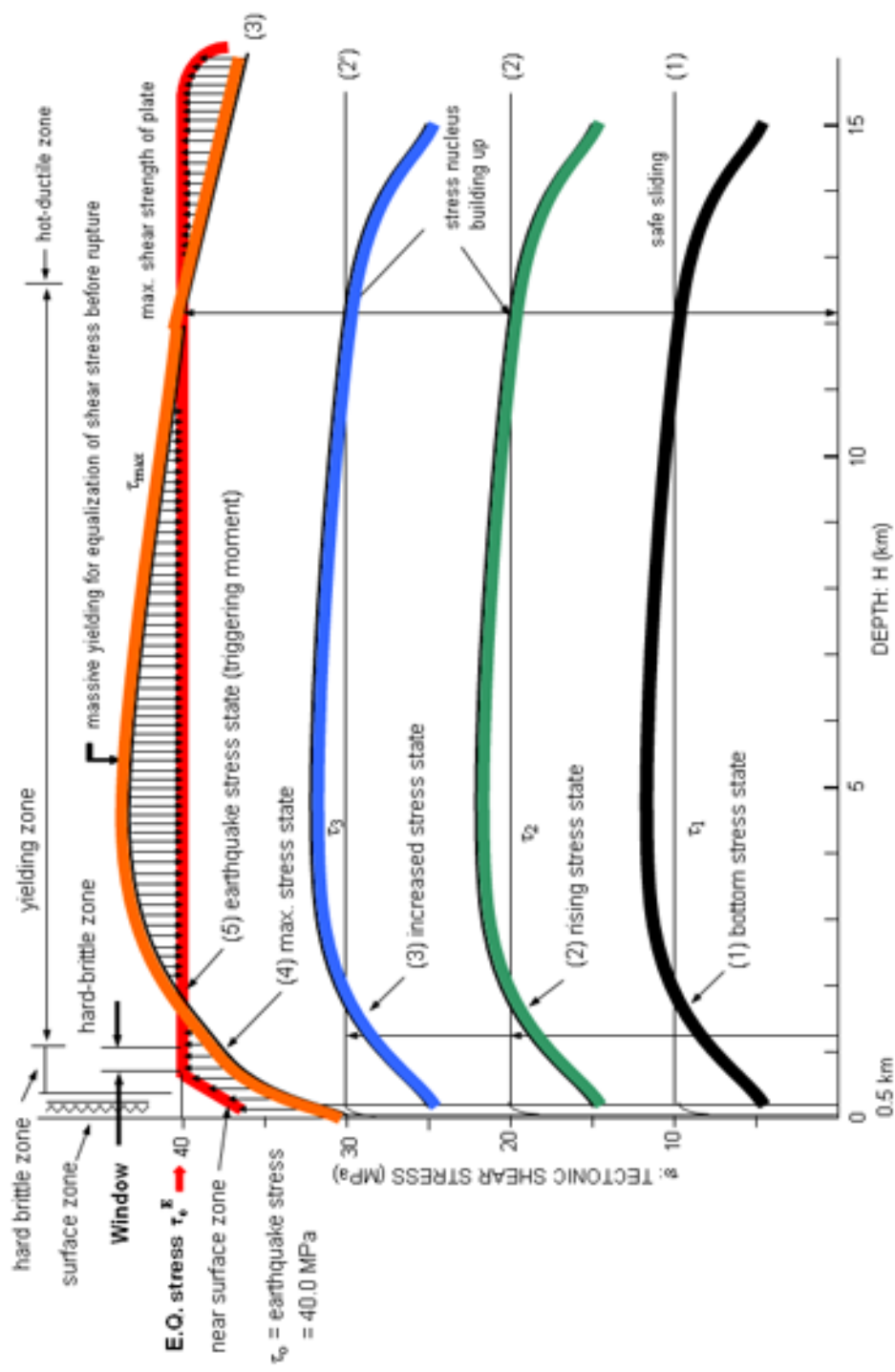


Fig. 5-12 Depth distributions of tectonic shear stress shown in relation to 5-stage earthquake stress cycle along major fault, illustrating stress nucleus yielding, resulting in the final equal shear stress state at the trigger moment. Most accurate earthquake prediction is made by continuous monitoring rise of Earthquake Stress Head at Window during the final stage of the cycle for accurate time-prediction

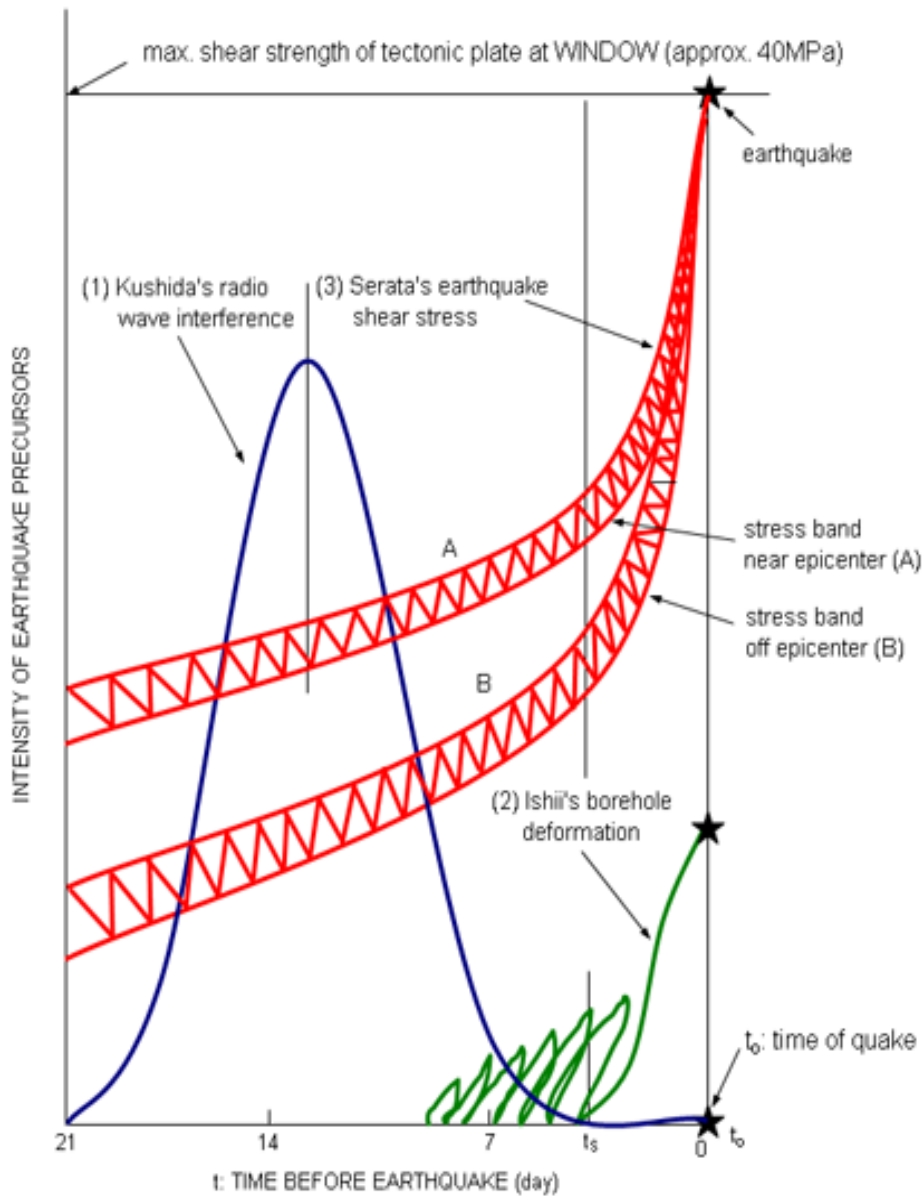
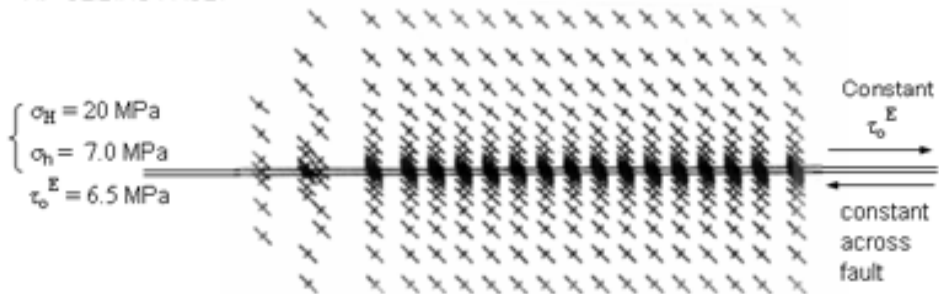
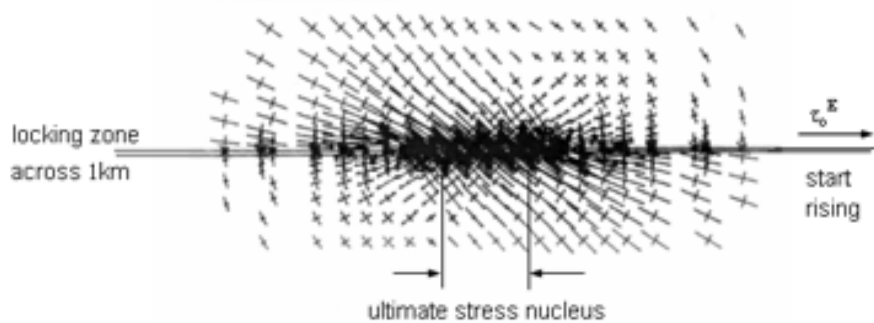


Fig. 5-13 Estimated time-prediction of forthcoming major earthquake made by dual monitoring of earthquake shear stresses τ_o^E on epicenter (A) and on near center (B) made by Serata Method (3), which is compared with Kushida's radio wave interference method (1) and Ishii's borehole micro deformation method (2)

A. SLIDING FAULT



B. START LOCKING



C. INCLINED STRESS MONITOR HOLE

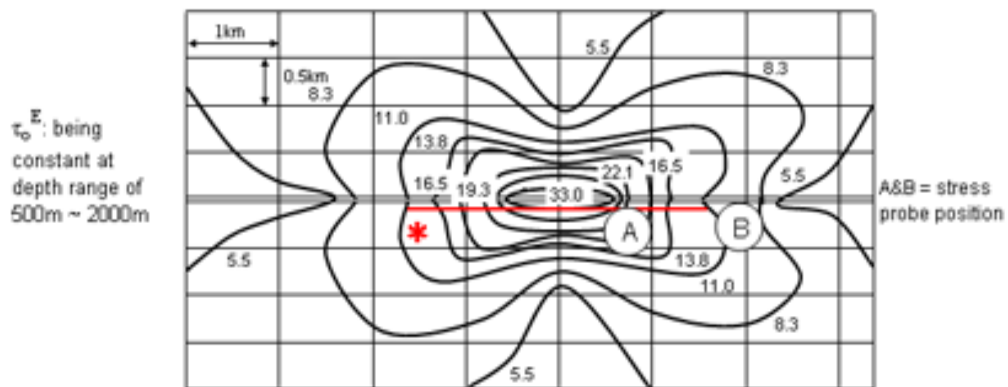


Fig. 5-14 Computer model analysis of earthquake stress (τ_0^E) build-up independent of depth at Window illustrating importance of stress monitoring test hole to be inclined in the plane (*) close and parallel to fault plane. This is to make τ_0^E measurements at varying distances from the epicenter A & B by utilizing one single inclined test hole.

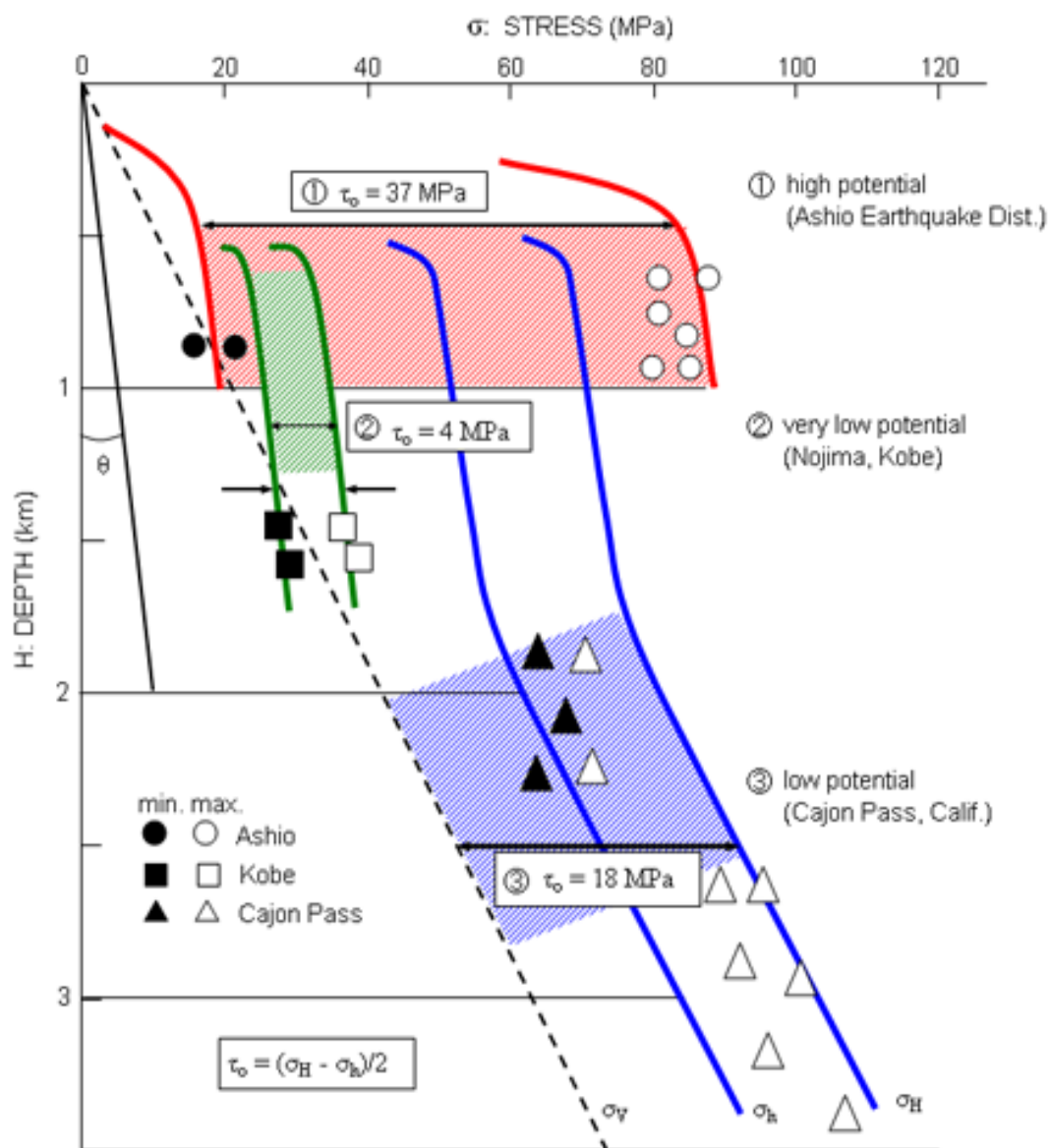


Fig. 5-15 Three different types of earthquake potential identified directly from stress measurements: (1) high earthquake potential (95%), (2) very low earthquake potential (10%) and (3) low earthquake potential (45%). The percentage indicates stress value relative to maximum strength. Data obtained from Annual Report of Japanese government (Environmental Protection Research Institute: Bosaiken, 2002)

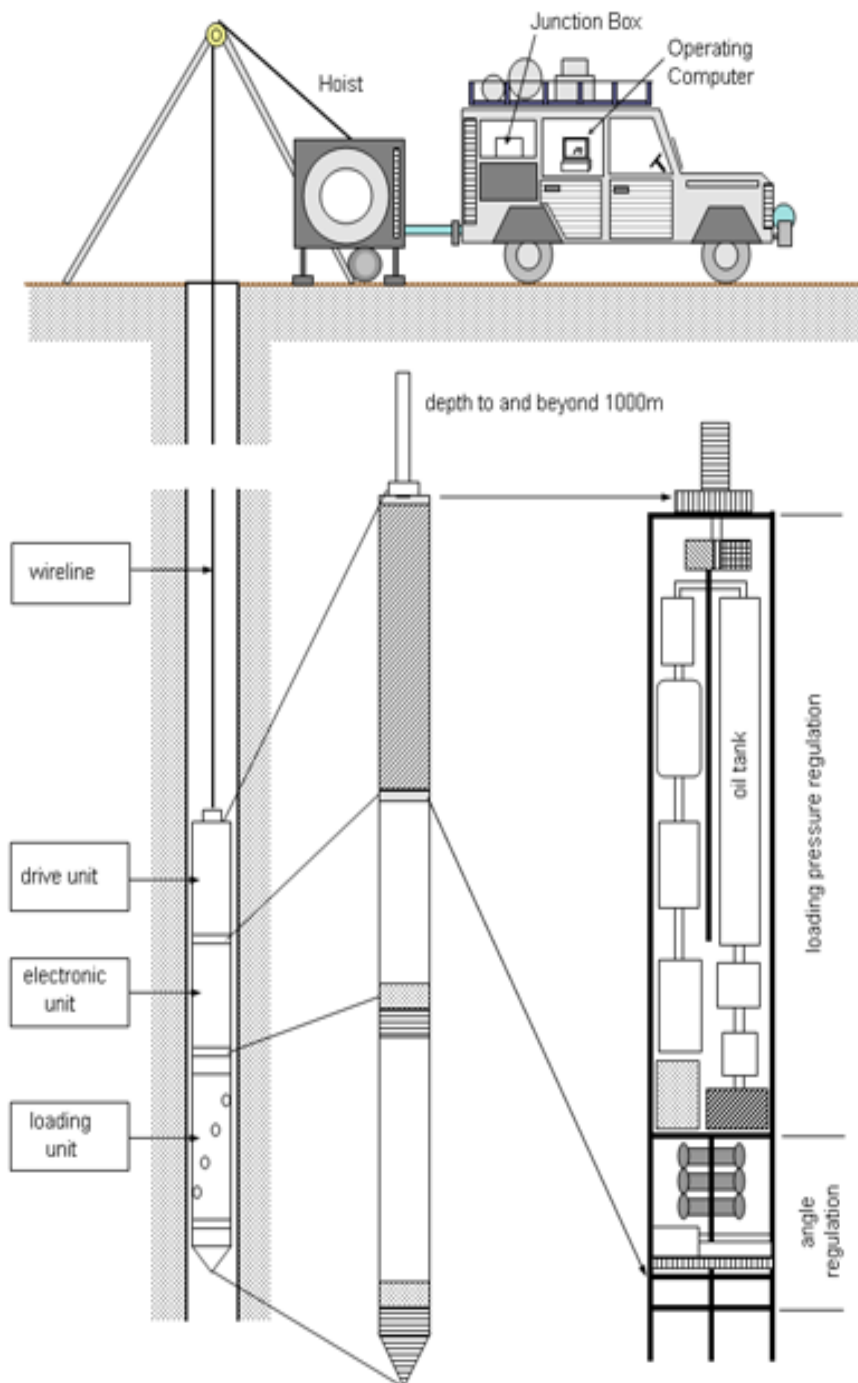


Fig. 5-16 Deep well remote operation system of Serata Probe



Fig. 5-17 Serata Probe used for automatic stress/property measurement to depth down to 1,000m accurately and repeatedly